

CASSON FLUID FLOW DUE TO STRETCHING SHEET WITH MAGNETIC EFFECT AND VARIABLE THERMAL CONDUCTIVITY

M. Y. Dhange^{a,*} G. C. Sankad^a, Ishwar Maharudrappa^b

^aDepartment of Mathematics, Research Centre (Affiliated to Visvesvaraya Technological University), BLDEA's V.P.Dr.P.G.Halakatti College of Engineering and Technology, Vijayapur, Karnataka 586 102, INDIA

^bDepartment of Mathematics, Basaveshwar Engineering College, Bagalkot, Karnataka 587 103, INDIA

ABSTRACT

The present paper investigates the impacts of heat transfer and magnetic field on the boundary layer flow of Casson fluid over a linearly stretching sheet. The researchers have introduced analytical and numerical solutions for the momentum and energy equations by transforming the equations into the system of ordinary differential equations with the aid of the similarity transformations technique. The velocity and temperature profiles for pertinent constraints like Casson fluid constraint, Chandrasekhar number, Prandtl number, and thermal conductivity are presented through graphs. The influence of the wall shear stress and the Prandtl number increases while the boundary layer thickness decreases. Further, the effects of the Casson fluid constraint on the local skin friction and thermal gradient are studied and the outcomes are presented in tabular form. It is also observed that increase in Casson fluid constraint and Chandrasekhar number the local skin friction coefficient also rises at the wall but decreases in the temperature at the wall. The outcomes revealed that the analytical method had a good agreement with the numerical solutions obtained through MATHEMATICA software. The current study has applications in the processing of magnetic materials and the extraction of crude petroleum from oil-based products.

Keywords: Boundary layer flow, linear-stretching sheet, Casson fluid, Chandrasekhar number, magnetohydrodynamics

1. INTRODUCTION

Most of the researchers are investigating in the direction of a steady flow of non-Newtonian fluid over a continuous linear/exponential stretching sheet, it has an extensive variety of applications in industrial processes such as resolidifying metallic products in freezing bath process, ejection of plastic films, to form polymer ply with the desired cross-section by forcing it through a dye. In the course of deposition of such polymer ply, the slit forms the blend that is subsequently stretched to give attentive thickness, and the sheet will solidify when it is moved through the cooling system to form well-graded output. It appears that the peculiarity of ply is the command by heat and mass transfer enclosed by the ply and fluid. The stretching sheet combines with the medium fluid thermally and mechanically during manufacture. Casson liquid is the most well-known non-Newtonian fluid that has a few applications in food handling, metal infection, boring tasks, and bio-designing activities. Sakiadis (1961) initiated an introduction of boundary layer flow over a continuous solid slab flowing at a constant rate. Crane (1970) has worked on a solution for two-dimensional incompressible boundary layer flow of adhesive fluid formed due to stretching plate.

Magyari and Keller (1999) solved the boundary layer flow problem over an exponentially stretching surface with ascending temperature diffusion analytically and numerically. Sajid and Hayat (2008) have worked on the analytic solution of boundary layer flow about Jeffrey fluid upon an exponential stretching plate. The model of MHD three-dimensional Casson liquid past a porous linearly stretched sheet was researched by Nadeem et al. (2012). Bhattacharya et al. (2013) elaborated on the effects of MHD boundary layer flow of Casson fluid overstretching and shrinking sheet with wall mass transfer through an

analytical solution. Mahanta and Shaw (2015) investigated three-dimensional Casson fluid flows via a porous linearly stretched sheet with convective boundary conditions using the Spectral Relaxation Method. The magneto-hydrodynamic stream across an exponentially overextended surface was studied by Emam and Elmaboud (2017). Pal and Mandal (2017) investigated nanofluid heat and mass transfer over a nonlinear stretching/shrinking sheet with viscous dissipation and thermal radiation using a double-diffusive magnetohydrodynamic heat and mass transfer model. The MHD flow and heat transfer characteristics of Williamson nanofluid due to a stretched sheet with variable thickness and thermal conductivity were investigated by Reddy et al. (2017). Sankad and Dhange (2017) explored the effect of wall features on the dispersion of a solute in the peristaltic motion of the Newtonian fluid. Aleng et al. (2018) analyzed a steady two-dimensional boundary layer flow of a nanofluid and heat transfer over a stretching/shrinking sheet. The Newtonian heating and convective boundary condition on MHD stagnation point flow past a stretching sheet with viscous dissipation and Joule heating were explored by Chaudhary et al. (2018). The influence of changing characteristics on the flow over an exponentially stretched sheet with convective heat conditions was studied by Srinivasacharya and Jagadeeshwar (2018). Irfan et al. (2019) analyzed the magnetohydrodynamic free stream and heat transfer of nanofluid flow over an exponentially radiating stretching sheet with variable fluid properties. Singh et al. (2019) studied mass transpiration in nonlinear MHD flow due to porous stretching sheets. Wakif (2020) has utilized a novel mathematical technique for MHD convective flows of Casson fluid over a nonlinear elastic sheet with temperature-dependent viscosity and thermal conductivity. Gangadhar et al. (2020) invent the fluid situations of boundary layer flow of Casson fluid over a nonlinearly stretching sheet with viscous dissipation. Haritha et al. (2020) presented an analytical

* Corresponding Author Email: math.mallinath@bldeacet.ac.in

solution for convective heat and mass transport of a rotating nano-fluid in a vertical conduit, which is bordered by extending and stationary walls. Ibrahim and Negera (2020) investigated the influence of thermal radiation and chemical reaction on the viscous dissipation of Williamson nanofluid over a stretching/shrinking wedge. Khan et al. (2020) took into account variable diffusion and conductivity changes in a 3D rotating Williamson fluid flow, as well as the magnetic field and activation energy. Reddy et al. (2020) reported the effect of heat absorption/generation on MHD Cu-water nanofluid stream above a non-linear shrinking/ stretching sheet. The influence of magnetized variable thermal conductivity on the flow and heat transfer characteristics of an unstable Williamson fluid was studied by Shankar et al. (2020). Shateyi and Muzara (2020) studied the unsteady MHD Blasius and Sakiadis flows with variable thermal conductivity in the presence of thermal radiation and viscous dissipation. The research of the MHD flow of Casson nanofluid across an infinite exponential porous surface in a rotating frame in the presence of slip velocity was explored by VeerKrishna et al. (2021). Ganesh and Sridhar (2021) explored the heat and mass transfer of an MHD Casson fluid under radiation with chemical reaction and Hall effects numerically using an exponentially permeable stretching sheet. Megahed et al. (2021) looked at the magnetohydrodynamic fluid flow caused by an unstable stretched sheet, thermal radiation, a porous material, and changing heat flux. Following these studies, a group of researchers looked into the boundary layer movement and stretching surface of a Casson fluid in a range of conditions involving convective heat and mass transfer flow (see Mukhopadhyay and Vajravelu (2013), Pramanik (2014), Ramesh and Devakar (2015), Animasaun et al. (2016), Maboob et al. (2017), Sampathkumar et al. (2021), Flihi et al. (2021), Goswami and Sarma (2021), Su et al. (2022), Yadhav and Choudhary (2022)).

With the above inspiration, in this manuscript, the Casson fluid boundary layer flow across a linearly stretched sheet is examined with the effects of heat transfer and magnetic field. The analytical and numerical solutions are provided the issues by transforming the momentum and energy equations into a system of ordinary differential equations using the similarity transformations technique. The effects of various diverse constraints on velocity and temperature profiles are deliberated briefly as well as displayed in terms of figures and tables.

2. METHODOLOGY

We consider the two-dimensional flow of an incompressible, steady non-Newtonian fluid caused by a stretching sheet. It coincides at $y = 0$, and the flow region refers to $y > 0$. The flow and heat transfer with radiation impacts are represented by the accompanying dimensional form of equations as (Abel et al. 2009, Mukhopadhyay and Vajravelu, 2013),

$$\frac{\partial u}{\partial x} + \frac{\partial v}{\partial y} = 0, \quad (1)$$

$$u \frac{\partial u}{\partial x} + v \frac{\partial u}{\partial y} = \nu \left(1 + \frac{1}{\beta} \right) \frac{\partial^2 u}{\partial y^2} - \frac{\sigma B_0^2 u}{\rho}, \quad (2)$$

$$u \frac{\partial T}{\partial x} + v \frac{\partial T}{\partial y} = \frac{K}{C_p} \frac{\partial^2 T}{\partial y^2}, \quad (3)$$

where u and v are the velocity components along x and y directions respectively, T is the temperature of the fluid, ρ is the density, σ is the electrical conductivity of the fluid, C_p is the specific heat at constant pressure, K is the thermal conductivity is assumed to vary linearly with temperature.

The associated boundary conditions for the present issue are:

- i. the velocity boundary conditions i.e. prescribed surface temperature (PST) are given by

$$u = a_0 x, v = 0,$$

$$T = T_w = T_\infty + A \left(\frac{x}{l} \right)^\lambda, \text{ when } y = 0, \quad (4a)$$

- ii. the temperature boundary conditions at an infinite distance away from the sheet is

$$u \rightarrow 0, T \rightarrow T_\infty \text{ as } y \rightarrow \infty. \quad (4b)$$

l is the sheets characteristic length, T_w is the temperature of the wall, T_∞ is the liquid temperature at an unlimited distance from the membrane, A is the constant of a dimensional wall, $a_0 (> 0)$ is the stretching rate.

Assumed that the convinced magnetic inclusion is negligibly small so that charge gained during the course is expanded on the ejection. To solve Eqs. (1)-(3), the similarity transformation is introduced as follows:

$$u = a_0 x f'(\eta), v = -\sqrt{a_0 \nu} f(\eta), \eta = \sqrt{\frac{a_0}{\nu}} y, \theta = \frac{T - T_\infty}{T_w - T_\infty}. \quad (5)$$

Equations (1)-(3) and the boundary conditions (4a) and (4b) take the following form:

$$\left(1 + \frac{1}{\beta} \right) f'''(\eta) = [f'(\eta)]^2 + q f'(\eta) - f(\eta) f''(\eta), \quad (6)$$

$$(1 + \epsilon \theta) \theta'' + P_r f(\eta) \theta' - \lambda P_r \theta f'(\eta) + \epsilon (\theta')^2 = 0, \quad (7)$$

$$\left. \begin{aligned} f(\eta) = 0, f'(\eta) = 1, \theta(\eta) = 1 \text{ at } \eta = 0 \\ f'(\eta) \rightarrow 0, \theta(\eta) \rightarrow \infty \text{ as } \eta \rightarrow \infty \end{aligned} \right\} \quad (8)$$

where β is the Casson fluid constraint, $q = \frac{\sigma B_0^2}{\rho a_0}$ is Chandrasekhar number, $P_r = \frac{\mu C_p}{k_\infty}$ is Prandtl number $k = k_\infty (1 + \epsilon \theta)$ is the thermal conductivity and $\epsilon = \frac{k_w - k_\infty}{k_w}$ is variable thermal conductivity coefficient, and λ is the temperature constant.

On solving Eqs. (6) and (7) by condition (8), we obtain a closed-form solution for the momentum as:

$$f(\eta) = \frac{1 - e^{-\alpha \eta}}{\alpha}, \text{ where } \alpha = \frac{\sqrt{\beta(1+q)}}{\sqrt{\beta+1}}. \quad (9)$$

The local skin friction coefficient is $f''(0) = -\alpha$ and it is determined for distinct values of the penetrating parameters.

By using the regular perturbation method, we have solved Eqs. (7) and (8). Let us assume that the exact solution of Eq. (7) in the form

$$\theta(\eta) = \theta_0(\eta) + \epsilon \theta_1(\eta) + \epsilon^2 \theta_2(\eta) + \epsilon^3 \theta_3(\eta) + \dots, \quad (10)$$

where $\theta_0(\eta)$, $\theta_1(\eta)$, $\theta_2(\eta)$, $\theta_3(\eta)$, ... are obtained as first, second, third, and so on order boundary value problems. The above sequence of BVP will be generated by using Eq. (10) in Eqs. (7) and (8) and then equating like powers of ϵ on both sides.

2.1 Zeroth order solution

The zeroth-order differential equation is

$$\epsilon \theta_0'' + \left\{ 1 - \frac{P_r}{\alpha^2} - \epsilon \right\} \theta_0' + 2\theta_0 = 0. \quad (11)$$

The boundary conditions are

$$\left. \begin{aligned} \theta_0(\epsilon_0) = 1 \text{ as } \epsilon_0 = -\frac{P_r}{\alpha^2} \\ \theta_0(\epsilon_0) \rightarrow 0 \text{ as } \epsilon_0 \rightarrow \infty. \end{aligned} \right\} \quad (12)$$

On transforming Eq. (11) into the confluent hypergeometric equation through suitable substitution and the solution in terms of Kummer's function as follows:

$$\theta_0(\eta) = b_0(\epsilon) \frac{P_r}{\alpha^2} M \left\{ \frac{P_r}{\alpha^2} - 2, \frac{P_r}{\alpha^2} + 1, \epsilon \right\}, \quad (13)$$

where $\epsilon = -\left(\frac{P_r}{\alpha^2}\right) e^{-\alpha \eta}$, M is Kummer's function, and

$$b_o = \frac{1}{(\epsilon)^{\frac{Pr}{\alpha^2}} M \left[\frac{Pr}{\alpha^2} - 2, \frac{Pr}{\alpha^2} + 1, \frac{-Pr}{\alpha^2} \right]}$$

2.2 First-order solution

The first-order differential equation is

$$\epsilon \theta_1'' + \left\{ 1 - \frac{Pr}{\alpha^2} - \epsilon \right\} \theta_1' + 2\theta_1 = -\{\epsilon \theta_o \theta_o'' + \theta_o \theta_o' + \epsilon (\theta_o')^2\}, \quad (14)$$

The boundary conditions are

$$\begin{aligned} \theta_1(\epsilon) &= 0 \quad \text{as } \epsilon_1 = -\frac{Pr}{\alpha^2} \\ \theta_1(\epsilon) &\rightarrow 0 \quad \text{as } \epsilon_1 \rightarrow \infty \end{aligned} \quad (15)$$

The solution of Eq. (14) with aid of border condition (15) is

$$\theta_1 = \theta_{11} + \theta_{12}, \quad (16)$$

where

$$\theta_{11} = c_o(\epsilon)^{\frac{Pr}{\alpha^2}} M \left\{ \frac{Pr}{\alpha^2} - 2, \frac{Pr}{\alpha^2} + 1, \epsilon \right\}, \quad (17)$$

$$c_o = \frac{-\sum d_r(\epsilon)^{r+2}}{(\epsilon)^{\frac{Pr}{\alpha^2}} M \left[\frac{Pr}{\alpha^2} - 2, \frac{Pr}{\alpha^2} + 1, \frac{-Pr}{\alpha^2} \right]}$$

$$\theta_{12} = \sum d_r \epsilon^{r+2}. \quad (18)$$

Since, ϵ is a however small quantity, after neglecting terms containing second and higher power in ϵ . The energy equation's primitive is in the form

$$\theta(\eta) = \theta_o(\eta) + \epsilon \theta_1(\eta). \quad (19)$$

The numerical solutions for the present study have also been completed by using MATHEMATICA software. The analytical and numerical solutions are presented in Table 1.

3. OUTCOMES AND DISCUSSION

To enlighten the importance of the present study, a set of numerical results for different parameters like the Casson fluid parameter (β), Chandrasekhar number (q), Prandtl number (Pr), temperature constant (λ) and the temperature variable coefficient (ϵ) on the flow, variables are plotted as shown in Figs. 1 - 6.

Figures 1 and 2 visualize the decrease in the velocity profile concerning several ascending values of Casson fluid parameter and Chandrasekhar number. The Chandrasekhar number is a dimensionless number used in magnetic convection to calculate the Lorentz power to viscosity ratio. Because the Chandrasekhar number is a fraction of the magnetic field and is proportional to the square of a typical magnetic field in a system, the velocity of fluid drops as the Casson fluid constraint and Chandrasekhar number increase.

The temperature profile for the distinct values of Chandrasekhar number, Prandtl number, temperature constant, and the temperature variable coefficient are shown in Figs. 3 - 6. Figure 3 displays the relation between the temperature and Chandrasekhar number, the emergent values of q is in the range (0.5, 1), there will be less reduction in the temperature. Further q increases from 1 to 2, and there is a rise in the temperature. The reason is that if $q < 1$ there is low magnetic intensity and high magnetic intensity when $q > 1$.

Figure 4 depicts that there is a loss in temperature growth for the increasing values of the temperature constant because of the exchange of heat between the sheet and the fluid. When the Prandtl number increases then the temperature decreases, due to this there is an augmentation in the speed of boundary layer thickness of the fluid model, and loss of heat enlargement (see Fig. 5). Figure 6 shows the temperature profile for increasing the values of the thermal conductivity variable coefficient constant. There is an enhancement in the temperature profile because the

constant coefficient of the thermal variable increases the magnitude of the temperature hence there will be growth in the heat flow.

In addition, we have put forth an attempt to extract (cf. Tab.1.) the effect of the Casson fluid parameter on the local skin friction coefficient ($-f''(0)$) and the thermal gradient ($-\theta'(0)$). From the table we induce that, for the progressive rising values of Casson fluid constraint and Chandrasekhar number, the local skin friction coefficient increases on the wall and there is a decline in the temperature gradient at the wall. Because the applied magnetic field creates a retarding force (Lorentz force) against the fluid's velocity, the drag is increased. The table shows the influence of the transverse magnetic field on heat transfer for the prescribed surface temperature (PST), and it can be seen that the transverse magnetic field adds to the thickening of the thermal boundary layer. The decrease in the temperature gradient is due to the resistance imposed by Lorentz's force on the flow of the Casson fluid.

4. CONCLUSIONS

The flow and heat transfer analysis of a two-dimensional unsteady hydromagnetic Casson fluid flow due to the linear stretching sheet is investigated. The heat flow is also discussed in the case of prescribed surface temperature (PST). The notable conclusions are as follows:

- The boundary layer thickness minimizes as Casson fluid constraint and Chandrasekhar number increase due to applied magnetic force.
- Ascends in the Casson fluid constraint lead to an increment in the local skin friction coefficient and a decrease in the temperature gradient.
- The boundary layer thickness decreases by increasing the values of the Prandtl number.
- As Casson fluid constraint assumes an infinity value, our results reduce to the case of a Newtonian fluid.
- The thermal variable coefficient constant can be used to maintain the magnitude of temperature in the flow.
- Numerically the temperature parameter determines the direction of heat transfer in the prescribed surface temperature (PST).

REFERENCES

- Abel, M.S., Datti, P.S., and Mahesha, N., 2009, "Flow and heat transfer in a power-law fluid over a stretching sheet with variable thermal conductivity and non-uniform heat source," *International Journal of Heat and Mass Transfer*, **52**, 2902-2913.
- Aleng, N.L., Bachok, N., and Arifin, N.M., 2018, "Dual solutions of exponentially stretched/shrunked flows of nanofluids," *Journal of Nanofluids*, **7**(1), 195-202.
- Animasaun, I.L., Adebile, E.A., and Fagbade, A.I., 2016, "Casson fluid flow with variable thermo-physical property along exponentially stretching sheet with suction and exponentially decaying internal heat generation using the homotopy analysis method," *Journal of Nigerian Mathematical Society*, **35**(1), 1-17. <https://doi.org/10.1016/j.jnnms.2015.02.001>
- Bhattacharyya, K., Hayat, T., and Alsaedi, A., 2013, "Analytic solution for magneto-hydrodynamic boundary layer flow of Casson fluid over a stretching/shrinking sheet with wall mass transfer," *Chinese Physics B*, **22**(2), 024702. <http://dx.doi.org/10.1088/1674-1056/22/2/024702>
- Chaudhary, S., Kanika, K.M., and Choudhary, M.K., 2018, "Newtonian heating and convective boundary condition on MHD stagnation point flow past a stretching sheet with viscous dissipation and Joule heating," *Indian Journal of Pure and Applied Physics*, **56**(2), 931-940.

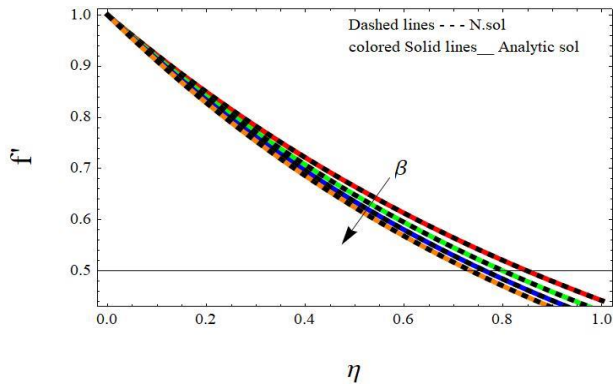


Fig 1. Velocity profile for distinct values of Casson fluid parameter $\beta = 0.5, 0.6, 0.7, 0.8$ with $q = 1$

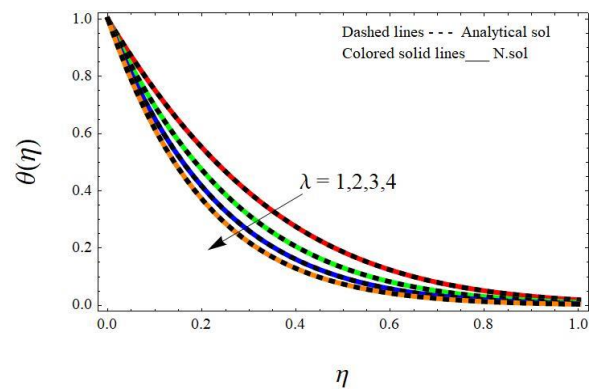


Fig 4. Temperature profile for different values of temperature constant $\lambda = 1, 2, 3, 4$ with $Pr = 6.2, q = 0.5, \beta = 1$.

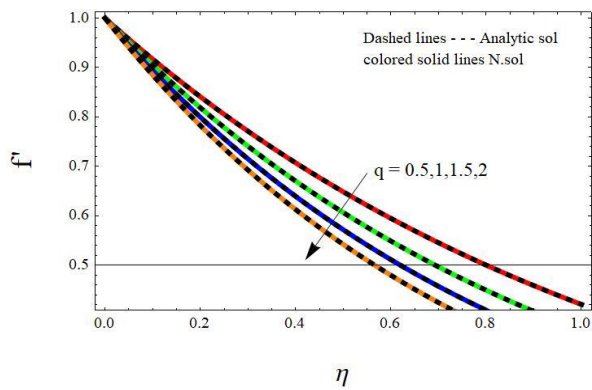


Fig 2. Velocity profile for distinct values of Chandrasekhar number $q = 0.5, 1, 1.5, 2$ with $\beta = 1$

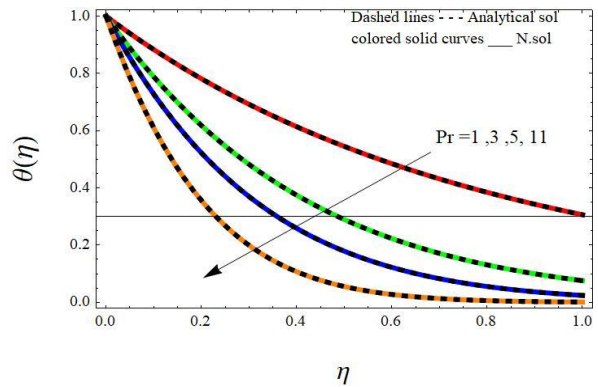


Fig 5. Temperature profile for different values of Prandtl number $Pr = 1, 3, 5, 11$ with $q = 1, \beta = 1$ and $\lambda = 2$.

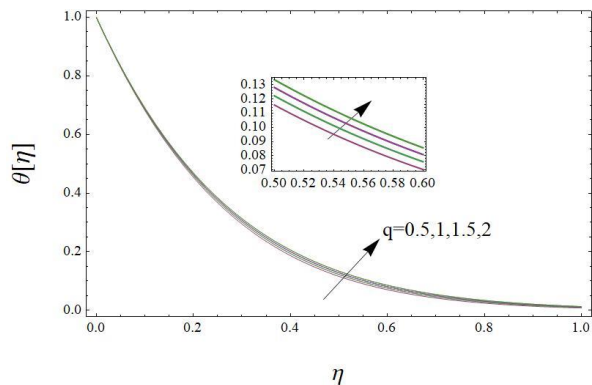


Fig 3. Temperature profile for different values of Chandrasekhar number with $\beta = 1, Pr = 6.2, \epsilon = 0.1,$ and $\lambda = 2$.

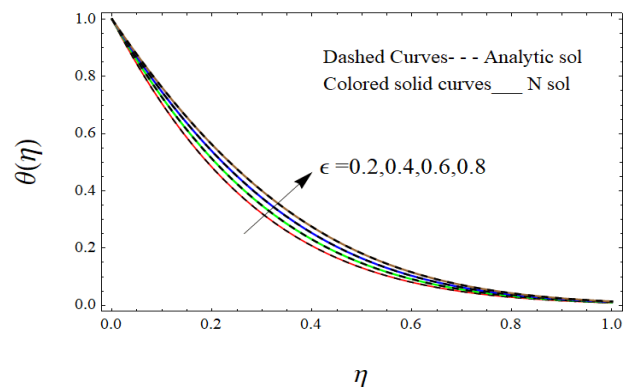


Fig 6. Temperature profile for different values of thermal variable coefficient $\epsilon = 0.2, 0.4, 0.6, 0.8$ with $Pr = 6.2, q = 0.5, \beta = 1$ and $\lambda = 2$

Table 1. Nature of local skin coefficient (α) and the temperature gradient ($-\theta'(0)$) for distinct values of Casson parameter (β) and Chandrasekhar number (q) with ($Pr = 1, \epsilon = 0.1, \lambda = 2$)

q	β	Analytical solution $\alpha = -f''(0)$	Numerical solution $\alpha = -f''(0)$	Perturbation solution $-\theta'(0)$	Numerical solution $-\theta'(0)$	q	β	Analytical solution $\alpha = -f''(0)$	Numerical solution $\alpha = -f''(0)$	Perturbation solution $-\theta'(0)$	Numerical solution $-\theta'(0)$
1	0.1	0.42640143	0.42640214	1.39450881	1.39450842	2	0.1	0.52223296	0.52223298	1.39450881	1.39450842
	0.2	0.57735025	0.57735027	1.35348185	1.35648105		0.2	0.70710678	0.70710677	1.35348185	1.35648105
	0.3	0.67936622	0.67936619	1.33023889	1.33023872		0.3	0.83205029	0.83205029	1.33023889	1.33023872
	0.4	0.75592894	0.75592892	1.31027914	1.31027911		0.4	0.92582009	0.92582009	1.31027914	1.31027911
	0.5	0.81649658	0.81649656	1.29432803	1.29432845		0.5	1.00000000	1.00000001	1.29432803	1.29432845
	0.6	0.86602540	0.86602540	1.28118347	1.28118363		0.6	1.06066017	1.06066017	1.28118347	1.28118363
	0.7	0.90748521	0.90748521	1.27011492	1.27011481		0.7	1.11143786	1.11143786	1.27011492	1.27011481
	0.8	0.94280904	0.94280904	1.26064049	1.26064056		0.8	1.15470053	1.15470053	1.26064049	1.26064056
	0.9	0.97332852	0.97332853	1.25242430	1.25242444		0.9	1.19207912	1.19207911	1.25242430	1.25242444
	1.0	1.00000000	1.00000000	1.24522263	1.24522290		1.0	1.22474487	1.22474487	1.24522263	1.24522290

Crane, L.J., 1970, "Flow past a stretching plate," *Journal of Applied Mathematics and Physics*, **21**, 645-647. <https://doi.org/10.1007/BF01587695>

Emama, T.G., and Elmaboud, T.A., 2017, "Three-dimensional magneto-hydrodynamic flow over an exponentially stretching surface," *International Journal of Heat and Technology*, **35**(4), 987-996.

Filihi, E., Sriti, M., Achemal, D., and EL Haroui, M., 2021, "CFD analysis of free convection in non-Darcian porous medium and comparison with similarity approach," *Frontiers in Heat and Mass Transfer*, **17.7**, 1-6. <https://doi.org/DOI:10.5098/hmt.17.7>

Gangadhar, K., Bhargavi, D.N., and Munagala, V.S.R., 2020, "Steady boundary layer flow of Casson fluid over a nonlinear stretched sheet in presence of viscous dissipation using the spectral relaxation method," *Mathematical Modeling in Engineering Problems*, **7**(3), 351-358. <https://doi.org/10.18280/mmep.070304>

Ganesh, G.R., and Sridhar, W., 2021, "Numerical approach of heat and mass transfer of MHD Casson fluid under radiation over an exponentially permeable stretching sheet with chemical reaction and hall effect," *Frontiers in Heat and Mass Transfer*, **16.5**, 1-11. <https://doi.org/DOI:10.5098/hmt.16.5>

Goswami, S., and Sarma, D., 2021, "The simultaneous effect of Eckert number and magnetic Prandtl number on Casson fluid flow," *Frontiers in Heat and Mass Transfer*, **16.12**, 1-7. <https://doi.org/DOI:10.5098/hmt.16.12>

Haritha, B., Umadevi, C., and Dhange, M., 2020, "Mathematical modeling of convective heat and mass transfer of a rotating nano-fluid bounded by stretching and stationary walls in a vertical conduit," *International Journal of Applied Mechanics and Engineering*, **25**(4), 69-83.

Ibrahim, W., and Negera, M., 2020, "Viscous dissipation effect on Williamson nanofluid over stretching/shrinking wedge with thermal radiation and chemical reaction," *Journal of Physics Communications*, **4**, 045015.

Irfan, M., Farooq, M.A., and Iqra, T., 2019, "Magneto-hydrodynamic free stream and heat transfer of nanofluid flow over an exponentially radiating stretching sheet with variable fluid properties," *Frontiers in Physics*, **7**, 186. <https://doi.org/10.3389/fphy.2019.00186>

Khan, M., Salahuddin, T., Yousaf, M.M., Khan, F., and Hussain, A., 2020, "Variable diffusion and conductivity change in 3D rotating Williamson fluid flow along with magnetic field and activation energy," *International Journal of Numerical Methods of Heat and Fluid Flow*, **30**(5), 2467-2484. <https://doi.org/10.1108/HFF-02-2019-0145>

Mabood, F., Khan, W.A., and Ismaila, A.I., 2017, "MHD flow over exponential radiating stretching sheet using homotopy analysis method," *Journal of King Saud University Engineering Sciences*, **29**(1), 68-74. <https://doi.org/10.1016/j.jksues.2014.06.001>

Magyari, E., and Keller, B., 1999, "Heat and Mass Transfer in the Boundary Layers on an Exponentially Stretching Continuous Surface," *Journal of Physics D: Applied Physics*, **32**, 577-585. <http://dx.doi.org/10.1088/0022-3727/32/5/012>

Mahanta, G., and Shaw, S., 2015, "3D Casson fluid flow past a porous linearly stretching sheet with convective boundary condition," *Alexandria Engineering Journal*, **54**(3), 653-659. <https://doi.org/10.1016/j.aej.2015.04.014>

Megahed, A.M., Ghoneim, N.I., Reddy, M.G., and El-Khatib, M., 2021, "Magneto-hydrodynamic fluid flow due to an unsteady stretching sheet with thermal radiation, porous medium, and variable heat flux," *Advances in Astronomy*, 2021(6686883), 1-9. <http://dx.doi.org/10.1155/2021/6686883>

Mukhopadhyay, S., and Vajravelu, K., 2013, "Diffusion of chemically reactive species in Casson fluid flow over an unsteady permeable stretching surface," *Journal of Hydrodynamics B*, **25**, 591-598. [https://doi.org/10.1016/S1001-6058\(11\)60400-X](https://doi.org/10.1016/S1001-6058(11)60400-X)

Nadeem, S., Haq, R.U., and Lee, C., 2012, "MHD flow of a Casson fluid over an exponentially shrinking Sheet," *Scientia Iranica*, **19**(6), 1550-1553. <https://doi.org/10.1016/j.scient.2012.10.021>

Pal, D., and Mandal, G., 2017, "Double diffusive magneto hydrodynamic heat and mass transfer of nanofluids over a nonlinear stretching/shrinking sheet with viscous-Ohmic dissipation and thermal radiation," *Propulsion and Power Research*, **6**(1), 58-69.

Pramanik, S., 2014, "Casson fluid flow and heat transfer past an exponentially porous stretching surface in presence of thermal radiation," *Ain Shams Engineering Journal*, **5**, 205-212.

Ramesh, K., and Devakar, M., 2015, "Some analytical solutions for flows of Casson fluid with slip boundary conditions," *Ain Shams Engineering Journal*, **6**(3), 967-975. <https://doi.org/10.1016/j.asej.2015.02.007>

Reddy, S.C., Naikoti, K., and Rashid, M.M., 2017, "MHD flow and heat transfer characteristics of Williamson nanofluid over a stretching sheet with variable thickness and variable thermal conductivity," *Transactions of A. Razmadze Mathematical Institute*, **171**, 195-211. <https://doi.org/10.1016/j.trmi.2017.02.004>

Reddy, Y.R., Rao, V.S., and Kumar, M.A., 2020, Effect of heat generation/absorption on MHD copper-water nanofluid flow over a non-linear stretching/shrinking sheet, *AIP Conference Proceedings*, 2246.

Sajid, M., and Hayat, T., 2008, "Influence of Thermal Radiation on the Boundary Layer Flow due to an Exponentially Stretching Sheet," *International Communications in Heat Mass Transfer*, **35**(3), 347-356.

Sakiadis, B.C., 1961, "Boundary-layer behavior on continuous solid surfaces: II The boundary layer on a continuous flat surface," *American Institute of Chemical Engineers*, **7**, 221-225. <http://dx.doi.org/10.1002/aic.690070211>

Sampathkumar, V.S., Pai, N.P., and Devaki, P., 2021, "Analysis of MHD flow and heat transfer of laminar flow between porous disks," *Frontiers in Heat and Mass Transfer*, **16**.3, 1-7. <https://doi.org/DOI:10.5098/hmt.16.3>

Sankad, G., and Dhange, M., 2017, "Effect of chemical reactions on the dispersion of a solute in peristaltic motion of Newtonian fluid with wall properties," *Malaysian Journal of Mathematical Sciences*, **11**(3), 347-363.

Shankar, U., Naduvnamani, N.B., and Hussain, B., 2020, "Effect of magnetized variable thermal conductivity on flow and heat transfer characteristics of unsteady Williamson fluid" *Nonlinear Engineering*, **9**(1), 338-351. <https://doi.org/10.1515/nleng-2020-0020>

Shateyi, S., and Muzara, H., 2020, "Unsteady MHD Blasius and Sakiadis flows with variable thermal conductivity in the presence of thermal radiation and viscous dissipation," *Frontiers in Heat and Mass Transfer*, **14**.18, 1-10. <https://doi.org/DOI:10.5098/hmt.14.18>

Singh, J., Mahabaleshwar, U.S., and Bognar, G., 2019, "Mass transpiration in nonlinear MHD flow due to porous stretching sheet," *Scientific Reports*, **9**, 18484.

Srinivasacharya, D., and Jagadeeshwar, P., 2018, "Effect of variable properties on the flow over an exponentially stretching sheet with convective thermal conditions," *Model. Meas. Control. B.*, **87**(1), 7-14. https://doi.org/10.18280/mmc_b.870102

Su, M., Kang, L., and Sun, K., 2022, "Numerical investigation for the laminar flow effects over rough surface using direction splitting," *Frontiers in Heat and Mass Transfer*, **18**.22, 1-5. <https://doi.org/DOI:10.5098/hmt.18.22>

VeerKrishna, M., Ameer, A.N., and Chamkha, A.J., 2021, "Radiative MHD flow of Casson hybrid nanofluid over an infinite exponentially accelerated vertical porous surface," *Case Studies in Thermal Engineering*, **27**, 101229. <https://doi.org/10.1016/j.csite.2021.101229>

Wakif, A., 2020, "A novel numerical procedure for simulating steady MHD convective flows of radiative Casson fluids over a horizontal stretching sheet with irregular geometry under the combined influence of temperature-dependent viscosity and thermal conductivity," *Mathematical Problems in Engineering*, **2021**(1675350), 1-20. <https://doi.org/10.1155/2020/1675350>

Yadhav, B.S., and Choudhary, S., 2022, "Effect of melting heat transfer and thermal radiation on squeezing flow of a Casson fluid with chemical reaction in porous medium," *Frontiers in Heat and Mass Transfer*, **18**.18, 1-10. <https://doi.org/DOI:10.5098/hmt.18.18>